공학석사 학위논문

Reduction of bone morphogenetic protein-2 dose through graphene oxide-based delivery for bone regeneration

그래핀 옥사이드 기반의 약물 전달을 통한 골형성 단백질 용량 감소 및 뼈 재생

2015 년 8 월

서울대학교 대학원

협동과정 바이오엔지니어링전공

정 문 주

Abstract

Reduction of bone morphogenetic protein-2 dose through graphene oxide-based delivery for bone regeneration

Moon-Joo Jung

Interdisciplinary Program for Bioengineering

The Graduate School

Seoul National University

High doses of bone morphogenetic protein-2 (BMP-2) are required for effective bone regeneration. However, these high doses often cause undesirable adverse effects, including bone overgrowth, osteolysis, and activation of the immune response, and raise treatment costs. In an effort to reduce the BMP-2 dose to avoid or diminish side effects, we investigated whether delivery of BMP-2 using graphene oxide (GO) can reduce the BMP-2 dose for bone regeneration. Delivery of BMP-2 using GO flakes suspended in fibrin gels (GO/F) resulted in significantly greater osteogenic differentiation of human bone marrow-derived mesenchymal stem cells in vitro, and at various doses of BMP-2, significantly greater amounts of bone regeneration in mouse calvarial defects occurred than when fibrin gel (F) alone was used. A half-dose of BMP-2 delivered by GO/F resulted in bone regeneration similar to that resulting from a full dose of BMP-2 delivered by F. The

enhanced bone regeneration efficacy was likely due, at least in part, to the sustained release, higher structural stability, and higher bioactivity of BMP-2 delivered by GO/F compared to BMP-2 delivered by F. Therefore, GO may be an effective carrier for BMP-2 to reduce the BMP-2 dose and avoid adverse effects.

Keywords: Bone morphogenetic protein-2, Bone regeneration, Fibrin, Graphene oxide

Student Number: **2013-21041**

Table of contents

Abstract ····· 1

Table of contents ····· 3

List of figures ····· 5

List of tables ····· 6

1. Introduction ····· 7

2. Materials and methods ····· 9

2.1. Cell culture ····· 9

2.2. GO characterization ····· 10

2.3. GO cytotoxicity assay ····· 11

2.4. BMP-2 adsorption on GO ····· 12

2.5. Release kinetics of BMP-2 ····· 13

2.6. Circular dichroism (CD) ····· 14

2.7. Osteogenic differentiation of hBMMSCs in vitro ····· 15

2.8. Quantitative real-time reverse transcriptase polymerase chain reaction (qRT-PCR) ····· 17

2.9. Western blot assay for cell signaling ····· 19

2.10. Mouse calvarial defect model for evaluating bone regeneration ····· 20

2.11. In vivo bone formation ····· 23

2.12. Statistical analysis ····· 24

3. Results ····· 25

3.1. GO characterization ····· 25
3.2. Cytotoxicity of GO ····· 27
3.3. BMP-2 adsorption on GO ····· 30
3.4. In vitro release of BMP-2 from GO and structural stability and bioactivity of the released BMP-2 ····· 33
3.5. In vitro osteogenic differentiation of hBMMSCs by released BMP-2 ····· 37
3.6. In vivo bone formation ····· 40
4. Discussion ····· 43
5. Conclusions ····· 46
References ····· 47
Supplementary data ····· 52
S1. Supplementary data experimental ····· 52
S1.1. Loading efficiency and release kinetics of bone morphogenic protein (BMP)-2 with various GO conditions ····· 52
S1.2. The compressive elastic modulus of F and GO/F ····· 54
S2. Supplementary data figures ····· 55
S3. Supplementary data references ····· 58
요약 (국문초록) ····· 59

List of figures

Figure 1. Characterization of the GO flakes ····· 26

Figure 2.1. Cytotoxicity of GO evaluated by neutral red assay ····· 28

Figure 2.2. Cytotoxicity of GO evaluated by TUNEL assay ····· 29

Figure 3.1. Adsorption of BMP-2 on GO. ····· 31

Figure 3.2. Raman spectroscopy of GO and BMP-2-adsorbed GO ····· 32

Figure 4.1. Sustained release of BMP-2 from GO/F versus F ····· 34

Figure 4.2. Higher structural stability of BMP-2 delivered by GO ····· 35

Figure 4.3. Higher bioactivity of BMP-2 delivered by GO ····· 36

Figure 5.1. Enhanced in vitro osteogenic differentiation of hBMMSCs cultured in the presence of BMP-2 released from GO/F ····· 38

Figure 5.2. Enhanced cell signaling related to osteogenic differentiation of hBMMSCs by BMP-2 delivered by GO, as evaluated by western blotting ····· 39

Figure 6.1. Bone regeneration evaluated by micro-CT. Representative micro-CT images of mouse skulls ····· 41

Figure 6.2. Bone regeneration evaluated by histological analysis with Goldner's trichrome staining of mouse calvarial defects ····· 42

List of tables

Table 1. Primer sequences used in qRT-PCR analysis to determine the level of gene expression for osteogenic differentiation and BMP-2 bioactivity ……18

1. Introduction

Bone morphogenetic proteins (BMPs) are potent bone-inducing factors [1]. Currently, BMP-2 and BMP-7 are being used clinically to regenerate bone [2-5]. High doses of BMP-2 are used in clinical treatment because it is rapidly lost from implanted carriers through diffusion and a short half-life [6,7]. However, high dosages raise the costs of treatment and often cause undesirable adverse effects. The clinical use of high-dose BMP-2 in spinal fusion has caused serious complications, such as ectopic bone formation [8], osteolysis [9], immune responses [8], post-operation neurological impairment [10], swelling at the surgery site [6,10], and airway compromise [8]. Therefore, reducing the dose of BMP-2 is necessary to avoid or diminish these complications.

The osteogenic efficacy, bioactivity, and optimal dosage of BMP-2 for bone formation are dependent on its delivery vehicle [11,12]. Therefore, an appropriate vehicle for BMP-2 delivery is required for effective bone formation. Appropriate delivery vehicles release BMP-2 locally at the bone-regeneration site over an extended period to avoid ectopic bone formation and induce effective bone formation [11,12]. A number of delivery vehicles have been evaluated for BMP-2 release. These carriers include collagen sponges [13], gelatin hydrogels [12], fibrin gel (F) [11,14], porous hydroxyapatite [15], poly(l-lactic-co-glycolic acid) (PLGA)/hydroxyapatite composite scaffolds [16], heparin-conjugated PLGA scaffolds [17], and heparin-conjugated PLGA nanospheres [18].

BMP-2 delivery using an appropriate vehicle may reduce the BMP-2 dose needed for bone regeneration. In the present study, we used graphene oxide (GO) flakes as a BMP-2 delivery vehicle. GO has been used as a delivery vehicle for

small-molecule drugs and genes because of its excellent biocompatibility, low toxicity, and large loading capacity [19,20]. Previously, we have used GO as a delivery vehicle for the BMP-2 protein [21]. GO is composed of hydrophobic domains in the core region and ionized groups along the edges. These features enhance its interactions with BMP-2 through hydrophobic and electrostatic interactions [21-23]. GO coated on titanium implants enabled the long-term release of BMP-2 with the retention of activity [21].

In the present study, we investigated whether delivery of BMP-2 using GO could reduce the BMP-2 dose needed for bone regeneration. BMP-2 was loaded on GO flakes, suspended in F (which has been frequently used as a bone formation scaffold and BMP-2 delivery vehicle [11]), and implanted in mouse calvarial defects to investigate the bone formation. The bone formation by BMP-2 delivery using GO flakes suspended in fibrin gels (GO/F) was compared to bone formation by F alone to determine whether delivery of BMP-2 using GO can reduce the BMP-2 dose needed for bone regeneration.

2. Materials and methods

2.1. Cell culture

Human bone marrow-derived mesenchymal stem cells (hBMMSCs) were purchased from Lonza (Lonza, Walkersville, MD, USA) and cultured with a growth medium that contained Dulbecco's Modified Eagle's Medium (DMEM, Gibco BRL, Gaithersburg, MD, USA) containing 10 % (v/v) fetal bovine serum (FBS, Gibco BRL) and 1 % (v/v) penicillin/streptomycin (PS, Pen Strep, Gibco BRL). The medium was changed every 2 days. For the experiments, hBMMSCs at four passages were used.

2.2. GO characterization

GO flakes were purchased from Sigma Aldrich (Product # 777676, Sigma, St. Louis, MO, USA) and examined by scanning electron microscopy (SEM, JSM-6701F, JEOL, Tokyo, Japan) after platinum coating. The size distribution of the GO flakes was determined with a dynamic light scattering spectrophotometer (DLS-7000, Otsuka Electronics, Osaka, Japan) and quantitative analysis of SEM images. The thickness of the GO flakes was determined using atomic force microscopy (AFM, Nanoscope IIIa, Digital Instrument, Santa Barbara, CA, USA) coupled with an inverted microscope (IX71 inverted microscope, Olympus, Tokyo, Japan).

2.3. GO cytotoxicity assay

GO flakes at various concentrations were added to the hBMMSC cultures, and the cells were cultured for 3 and 7 days. Cell viability was evaluated using the Neutral Red assay as described previously [24]. The absorbance of the sample were expressed as a percentage of the positive control (no GO) value (n = 5 for each group). A terminal deoxynucleotidyl transferase dUTP nick end labeling (TUNEL) assay was performed to determine the apoptotic activity of hBMMSCs cultured with or without GO (200 ng/ml) using an ApopTag Red in situ apoptosis detection kit (Millipore, Billerica, MA, USA) according to the manufacturer's instructions. The percentage of TUNEL-positive cells was determined by dividing the number of TUNEL-positive-cells by the number of DAPI (Vector Laboratories, Burlingame, CA, USA)-positive cells. Thirty different pictures were randomly selected from each group for the calculations.

2.4. BMP-2 adsorption on GO

GO flakes were labeled with 1,1'-dioctadecyl-3,3,3'3'-testramethylindocarbocyanine perchlorate (DiI, red, Sigma) prior to BMP-2 adsorption. For BMP-2 adsorption, fluorescein isothiocyanate (FITC, green, Thermo Scientific, Rockford, IL, USA)-conjugated BMP-2 (Cowell Medi Co., Busan, South Korea) and DiI-labeled GO was added to phosphate-buffered saline (PBS) and incubated for 4 h at 4 C. The weight ratio of GO to BMP-2 was 1:1. BMP-2 adsorbed on GO was visualized using fluorescence microscopy (IX71 inverted microscope, Olympus). The BMP-2 adsorption ratio was determined by quantifying the amounts of total BMP-2 and non-adsorbed BMP-2 with a fluorescence spectrometer (FP-777, Jasco, Tokyo, Japan). To confirm BMP-2 adsorption on GO, Raman spectra were acquired using a Renishaw Raman spectrometer (Renishaw, New Mills, Gloucestershire, UK) with 514.5 nm wavelength incident laser light.

2.5. Release kinetics of BMP-2

The release profiles of BMP-2 from GO/F or BMP-2 released from F alone were determined by enzyme-linked immunosorbent assays (ELISAs, R&D Systems Inc., Minneapolis, MN, USA) [8]. To determine the BMP-2 loading on GO, BMP-2 (1 g) was added to 20 l of PBS containing GO and incubated for 4 h at 4 C. Following incubation, an ELISA of the supernatant showed that all the BMP-2 was adsorbed on the GO. F kits (Greenplast) were purchased from GreencrossPD Co. (Yongin, Kyunggi-do, South Korea). F was prepared by mixing fibrinogen (100 mg/ml) dissolved in aprotinin (100 KIU/ml) solution with thrombin (500 IU) dissolved in calcium chloride solution (6 mg/ml). The BMP-2-loaded GO was suspended in 0.5 ml of F and immersed in a 2-ml microcentrifuge tube containing 1.5 ml of PBS. The tubes were then incubated at 37 C with continuous agitation. At various time points, the supernatant was collected, and fresh buffer was added to the microcentrifuge tubes. The concentration of BMP-2 in the supernatant was determined by ELISA.

2.6. Circular dichroism (CD)

The structure of BMP-2 protein adsorbed onto the GO surface after 3 days of incubation in PBS at room temperature was examined using CD (Jasco J-810, Applied Photophysics, Surrey, UK) and compared to the structure of native BMP-2. The structure of free BMP-2 protein incubated in PBS for 3 days at room temperature was also examined. The BMP-2 adsorbed on the GO was detached by centrifugation at 12,000 rpm for 10 sec. The BMP-2 content was quantified using Bradford reagent (Sigma). Each CD spectrum and its corresponding high-tension voltage curve were recorded on a Jasco J-810 spectropolarimeter using a quartz cell with an optical path length of 1 mm. The scanning speed was set at 50 nm/min, and the wavelength range was set at 180260 nm. The ratio of the -helix in BMP-2 was determined using CDNN secondary structure analysis software (Applied Photophysics).

2.7. Osteogenic differentiation of hBMMSCs in vitro

For alkaline phosphatase (ALP) activity evaluation, calvarial osteoblasts were isolated from the calvaria of neonatal (less than 1 day old) Sprague-Dawley rats (SLC, Tokyo, Japan) by a digestive enzymatic process [11]. Rat calvarial osteoblasts (3104 cells per well) were plated in six-well tissue culture plates (Corning, Corning, NY, USA). Delivery vehicle containing 2 g of BMP-2 was placed on culture inserts (Transwell, Corning) in the culture plates. The culture medium was DMEM (Gibco) containing 10 % (v/v) FBS (Gibco) and 1 % PS (Gibco). The medium was changed every 3 days. The ALP activity was determined using p-nitrophenol phosphate (Anaspec, San Jose, CA, USA) as the substrate. The cultured rat calvarial osteoblasts were rinsed twice with PBS and lysed in alkaline lysis buffer, followed by three freeze-thaw cycles that involved serial exposure to 70 C and 37 C. The samples were incubated in glycine buffer containing 2 mg/mL of p-nitrophenol phosphate. After 30 min, 3 N NaOH was added to stop the reaction. The absorbance of p-nitrophenol phosphate was measured at 405 nm. The total amount of cellular protein was determined using Bradford reagent (Sigma). The enzyme activity was then normalized relative to the total amount of cellular protein. The experiments were performed in triplicate.

To evaluate osteogenic differentiation of hBMMSCs induced by BMP-2, hBMMSCs were cultured for 2 weeks with or without F or GO/F that was loaded with BMP-2 (2 g per well) and placed in the transwell inserts. As a positive control, BMP-2 was added daily to the osteoblast culture at the same concentration as that of BMP-2 released from the GO/F. The hBMMSCs were stained immunocytochemically with antibodies against osteocalcin (OC, Abcam, Cambridge, MA, UK). The staining signal was visualized using FITC-conjugated

secondary antibodies (Jackson Immuno Research Laboratories, West Grove, PA, USA). The slides were counterstained with DAPI (Vector Laboratories) to stain the cell nuclei and were photographed after visualization with a fluorescence microscope (Olympus).

2.8. Quantitative real-time reverse transcriptase polymerase chain reaction (qRT-PCR)

qRT-PCR was performed to determine the relative quantities of mRNA expression for various genes. All qRT-PCR reactions were performed using a Light Cycler 480 (Roche, Basel, Switzerland) and SYBR Green I (TAKARA, Shiga, Japan). After 5 min of pre-incubation at 90 C, 35 amplification cycles were performed. Each cycle consisted of the following three steps: 30 seconds at 94 C, 45 seconds at 60 C, and 45 seconds at 72 C. The sequences of the primers used for qRT-PCR are shown in Table 1.

Table 1. Primer sequences used in qRT-PCR analysis to determine the level of gene expression for osteogenic differentiation and BMP-2 bioactivity.

Gene	Primer
GAPDH	sense 5’- GTC GGA GTC AAC GGA TTT GG -3’ antisense 5’- GGG TGG AAT CAA TTG GAA CAT -3’
OC	sense 5’- CCT CAC ACT CCT CGC CCT ATT -3’ antisense 5’- ATG ACG ATG GAC AAG TAC CC -3’
ALP	sense 5’- CCC TTG ACC CCC ACA ATG T -3’ antisense 5’- GTT GTT CCT GTT CAG CTC GTA -3’
OP	sense 5’- ACC AGC CCA ACA ACA CTC CT -3’ antisense 5’- AGC TGA AAT GGA CTT CCT GGT C -3’

2.9. Western blot assay for cell signaling

Western blotting was performed to evaluate the molecular signaling in the osteogenic differentiation of hBMMSCs cultured for 2 weeks with or without F or GO/F loaded with BMP-2 (2 μg per well). The cell suspension was centrifuged at 4 ℃ and 15,000 g for 10 min. The cells were resuspended in cold lysis buffer (50 mM TrisHCl, pH 8.0, 150 mM NaCl, 1 % Nonidet P-40) containing a protease inhibitor cocktail for 30 min. The protein extracts were clarified by centrifugation at 4 ℃ and 15,000 g for 30 min. The protein extracts were loaded onto gels for SDS-PAGE and separated by electrophoresis. The gels were then transferred to a nitrocellulose membrane using an iBLOT system (Invitrogen, Carlsbad, CA, USA). The membrane was blocked with 5 % skim milk in Tris buffered saline with Tween 20 (TBST) at room temperature for 1 h and then incubated with primary antibody at room temperature for 1 h. The membrane was washed five times (10 min each) and then incubated with horseradish peroxidase-conjugated anti-mouse or rabbit antibody in TBST for 30 min. Immunoreactivity was visualized using enhanced chemiluminescence.

2.10. Mouse calvarial defect model for evaluating bone regeneration

A mouse calvarial defect model was produced as previously described [14]. Six-week-old mice from the Institute of Cancer Research (Koatech, Sungnam, Kyunggi-do, South Korea) were anesthetized with xylazine (20 mg/kg) and ketamine (100 mg/kg). After the scalp hair was shaved, a longitudinal incision was made in the midline of the cranium from the nasal bone to the posterior nuchal line, and the periosteum was elevated to expose the surface of the parietal bones. Using a surgical trephine burr (Ace Surgical Supply Co., Brockton, MA, USA) and a low-speed micromotor, 2 circular transosseous defects (diameter, 4 mm) per mouse were produced in the skull. The defect size corresponded to the critical defect size for the mouse calvarial defect model [14]. The drilling site was irrigated with saline, and the bleeding points were electrocauterized. Five animals (10 defects) were used in each group. The calvarial defects were filled with F (50 μl) or GO/F with or without BMP-2 (0, 0.3, 0.5, and 1.0 μg/implant). The skin was then closed with resorbable 6-0 Vicryl sutures (Ethicon, Edinburgh, UK). The animal study was approved by the Institutional Animal Care and Use Committee at Seoul National University (#120305-5).

GO/F was implanted with the weight ratio of BMP-2 to GO of 1:1. To enhanced bone regeneration efficiency in vivo, the weight ratio of BMP-2 to GO, thickness and size of GO, and oxidation degree of GO were considered. We used the 1:1 weight ratio of GO to BMP-2 in the animal study because we concerned about loading efficiency of BMP-2 on GO and cytotoxicity of GO for effective bone regeneration. The weight ratio of BMP-2 to GO of 1:1 showed higher loading efficiency than 1:0.1 weight ratio when the amount of BMP-2 was fixed to 1 μg

(Fig. S1). We investigated the loading efficiency of BMP-2 on GO at two different weight ratios of BMP-2 to GO. 1 μg of BMP-2 was used in our in vivo bone regeneration study, and was loaded on 0.1 μg of GO (1:0.1 weight ratio of BMP-2 to GO) or 1 μg of GO (1:1 weight ratio of BMP-2 to GO). The loading efficiency of BMP-2 on GO was enhanced with increased GO amount as shown in supplementary data figure 1. Also, the amount of GO used in our in vivo bone regeneration study was 1 μg (20 μg/ml fibrin). A previous study reported that GO did not show cytotoxicity when GO concentration was increased up to 100 μg/ml [25]. Compared to the previous study, the GO concentration used in our experiments (1:1 weight ratio of GO to BMP-2, fixed BMP-2 amount = 1 μg, GO amount = 1 μg) would be non-toxic. The amount of BMP-2 loaded on GO is critical for bone regeneration in vivo. As shown in supplementary data figure 1, the weight ratio of BMP-2 to GO of 1:1 showed higher efficiency of BMP-2 loading than 1:0.1 when the amount of BMP-2 was fixed to 1 μg. This result demonstrated that higher amount of BMP-2 could be loaded on GO when the weight ratio of BMP-2 to GO was 1:1 than 1:0.1. Therefore, the bone regeneration efficiency in vivo would be enhanced when the weight ratio of BMP-2 to GO of 1:1 is used for bone regeneration than using the weight ratio of BMP-2 to GO is 1:0.1. The loading efficiency of BMP-2 on GO would not be affected by thickness of GO since BMP-2 binds to the π-π interaction-possible surfaces of GO [21]. A previous study demonstrated that the loading efficiency of protein on GO was not affected by the size of GO at the same thickness and amount of GO [26]. The GO used in our experiments was purchased from Sigma-Aldrich. Sigma-Aldrich does not open the synthetic methods and experimental parameters to the public. We reduced GO instead of increasing the oxidation degree of GO, since it is very difficult to

increase the oxidation degree of already synthesized GO. To produce the GO with increased oxidation degrees, GO should be modified from the initial synthesizing steps. Therefore we were not able to produce the GO with increased oxidation degrees. We reduced GO using ascorbic acid and investigated the loading efficiency of BMP-2 on GO with two different oxidation degrees (i.e., GO versus Reduced GO) and release profiles of BMP-2 for 3 weeks. The loading efficiency of BMP-2 on GO was decreased with decreased oxidation degree of GO. However, the release profile of BMP-2 from GO was not changed by the oxidation degree (Fig. S2).

2.11. In vivo bone formation

Eight weeks after implantation, the mice were sacrificed and the implants were retrieved and fixed in 4 % paraformaldehyde. Bone formation was evaluated using microcomputed tomography (micro-CT) scanning (SkyScan-1172, Skyscan, Kontich, Belgium) and histological analysis. The micro-CT system was operated at a voltage of 40 kV and a current of 250 mA. For the histological analysis, the specimens were embedded in paraffin and sectioned transversely to obtain 4-mm-thick sections; the sections were examined after Goldner's trichrome staining. The area of bone formation was measured using an image analysis system coupled to a light microscope. The bone formation area was expressed as the percentage of bone area in the total cross-sectional area [(bone area/total area) x 100 %] [27].

2.12. Statistical analysis

Quantitative data were expressed as the mean ± standard deviation. For the statistical analysis, a one-way analysis of variance (ANOVA) with Bonferroni test was performed using the OriginPro 8 SR4 software package (ver. 8.0951, OriginLab Corporation, Northampton, MA, USA). The assumptions of ANOVA to satisfy Levene's test for homogeneity of variance and to pass test for normality were found. $p < 0.05$ was considered to be statistically significant.

3. Results

3.1. GO characterization

A SEM showed that the GO flakes were rectangle-shaped sheets (Fig. 1A). The average size of the GO flakes by quantitative analysis of SEM images was 1.8 μm (Fig. 1A). The size distribution of the GO flakes was measured by laser light scattering (Fig. 1B). AFM revealed that the GO flakes had various sizes and were approximately 3 nm thick (Fig. 1C).

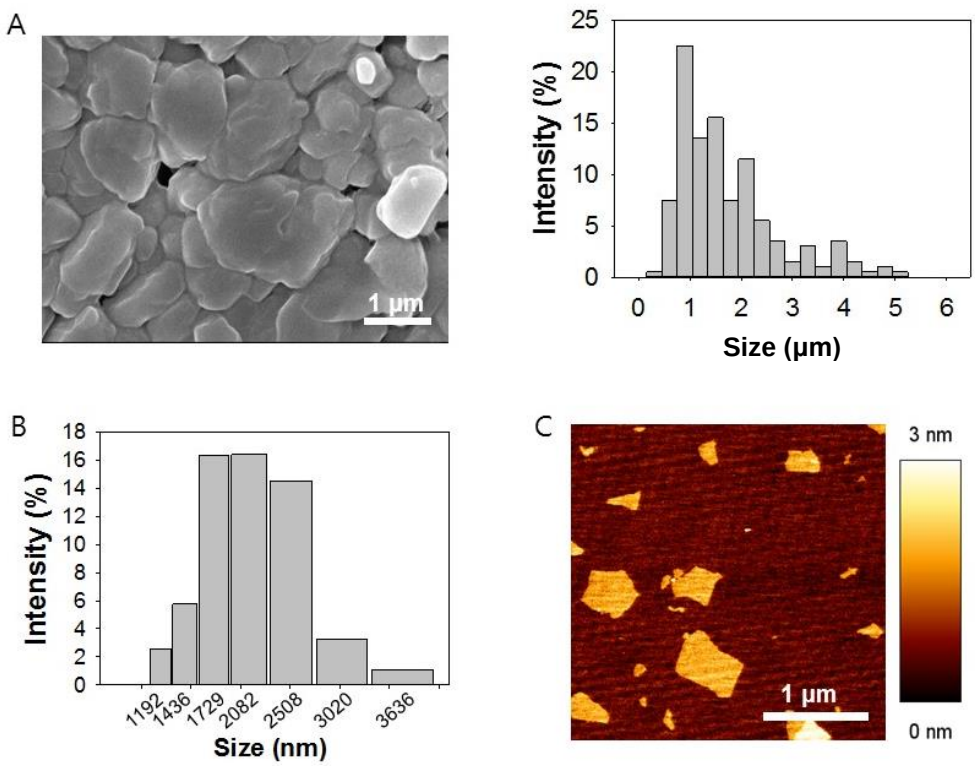

Figure 1. Characterization of the GO flakes. (A) SEM image of the GO flakes and quantitative analysis of SEM images. Scale bar = 1 μm. (B) The size distribution of GO flakes as determined by laser light scattering. (C) AFM image of the GO flakes. Scale bar = 1 μm.

3.2. Cytotoxicity of GO

The GO flakes showed dose-dependent cytotoxicity, as evaluated by neutral red assay (Fig. 2.1A). At 3 days, the GO showed negligible cytotoxicity at 10, 20, 40, 60, 80 and 100 μg/ml concentrations. However, at day 7, the GO showed dose-dependent cytotoxicity. Many hBMMSCs (20~45 %) were dead at day 7 with GO concentrations of 10, 20, 40, 60, 80, and 100 μg/ml. GO concentrations higher than 10 μg/ml were cytotoxic. However, at 200 ng/ml, GO was not cytotoxic because there was no difference in the viability of hBMMSCs cultured with or without 200 ng/ml GO for 7 days (Fig. 2.1B). The TUNEL assay indicated that 200 ng/ml GO did not induce apoptosis during the culture period of 7 days (Fig. 2.2). No cells were TUNEL-positive at 200 ng/ml GO at day 7.

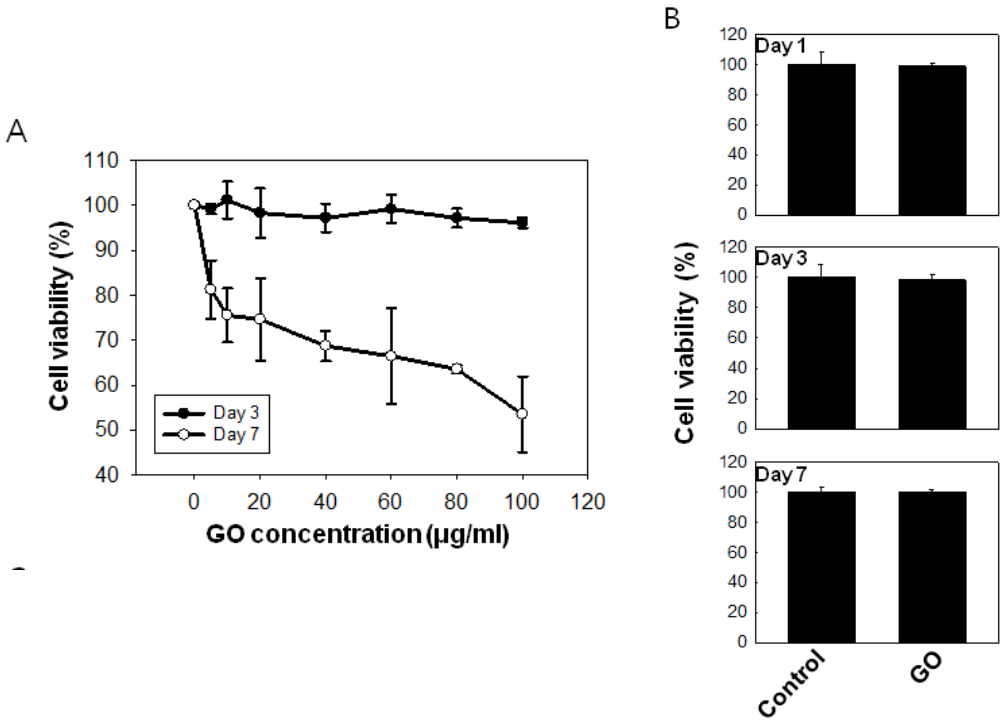

Figure 2.1. Cytotoxicity of GO. (A) Viability of hBMMSCs cultured for 3 or 7 days in the presence of various concentrations of GO flakes, as determined by the neutral red assay. (B) Viability of hBMMSCs cultured for 1, 3, or 7 days with or without GO flakes (200 ng/ml), as determined by the neutral red assay

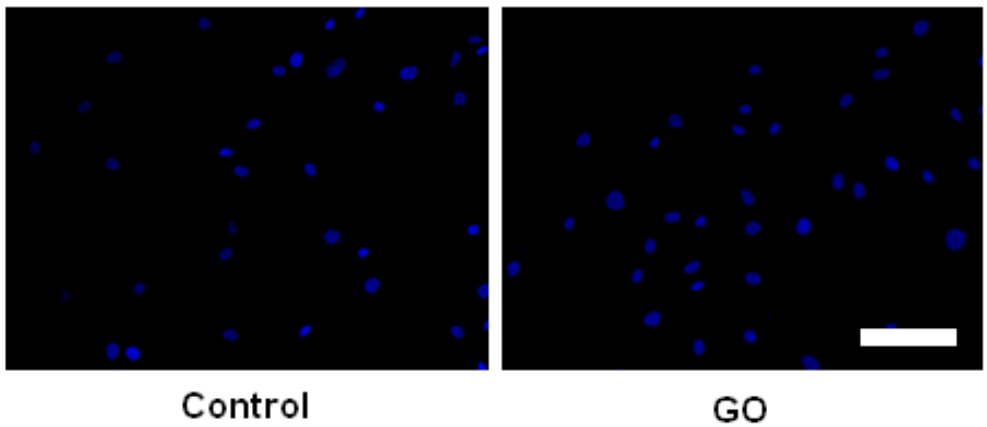

Figure 2.2. Cytotoxicity of GO. Apoptotic activity of hBMMSCs cultured with or without GO (200 ng/ml) for 7 days. Apoptotic cells (red) were stained in the TUNEL assay. Nuclei were counterstained with DAPI (blue). The images were obtained at the same magnification (x 100). Scale bars = 100 μm.

3.3. BMP-2 adsorption on GO

Following incubation of DiI (red)-labeled GO and FITC (green)-conjugated BMP-2 in PBS for 4 h, BMP-2 was adsorbed on GO (Fig. 3.1). The BMP-2 adsorption ratio was determined by quantifying the amounts of total BMP-2 and non-adsorbed BMP-2 by fluorescence spectrometry. The analysis revealed that 90.0 ± 3.3 % of total BMP-2 was adsorbed on GO after 4 h. This result indicates that GO adsorbs BMP-2 protein well. Raman spectroscopy also showed BMP-2 adsorption on GO (Fig. 3.2). In the GO spectrum, the peak at 1580 cm−1 (G-band) corresponds to an E2g mode of graphite and is related to the vibration of sp2-bonded carbon atoms in a 2D hexagonal lattice [28]. The peak at 1350 cm−1 (D-band, the breathing mode of A1g symmetry) is associated with vibrations of carbon atoms with dangling bonds in plane terminations of disordered graphite. The GO-specific carbon peaks decreased after BMP-2 adsorption on GO, indicating the reduction in size of the inplane sp2 domains due to the adsorption of BMP-2.

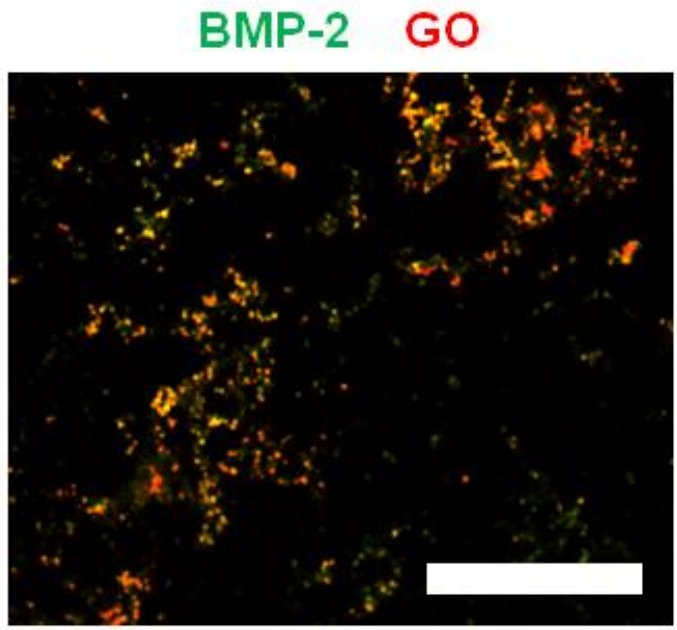

Figure 3.1. Adsorption of BMP-2 on GO. Fluorescence microscopy image of FITC (green)-conjugated BMP-2 adsorbed on DiI-labeled GO (red) after 4 h of incubation and subsequent washing with PBS three times. Scale bars = 50 μm.

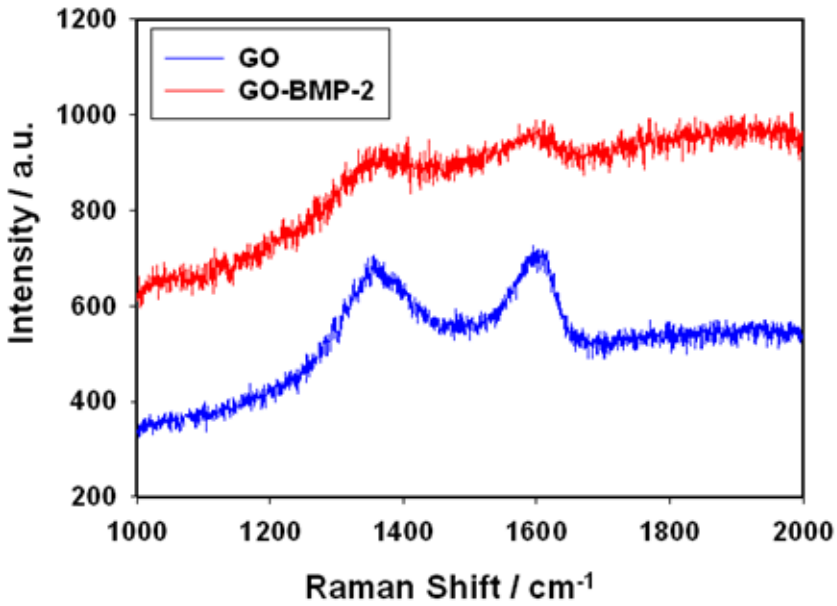

Figure 3.2. Raman spectroscopy of GO (blue) and BMP-2-adsorbed GO (red).

3.4. In vitro release of BMP-2 from GO and structural stability and bioactivity of the released BMP-2

BMP-2 was released from GO in a sustained manner. The profiles of in vitro release of BMP-2 from F or GO/F were compared (Fig. 4.1). The GO/F delivery vehicle exhibited a slower release of BMP-2 compared with F alone. Compared to the GO/F carrier, the F carrier showed an initial burst of BMP-2 release. Approximately 84 % of the BMP-2 loaded in F was released over the first 3 days, whereas the same dose of BMP-2 was released from GO/F over a period of 13 days. BMP-2 adsorbed on GO had a CD spectrum similar to that of native BMP-2 even after three days of adsorption (Fig. 4.2A). In contrast, the CD spectrum of free BMP-2 incubated in PBS for 3 days showed more structural denaturation of the protein. The α-helix content of the GO-adsorbed BMP-2 was significantly higher than that of free BMP-2 in PBS (Fig. 4.2B). The bioactivity of BMP-2 released from the carriers was evaluated by determining the ALP activity of rat osteoblasts cultured in the presence of the released BMP-2 (Fig. 4.3A) [21]. The ALP activity was significantly higher in the GO/F/BMP-2 group than in the F/BMP-2 group at days 11 and 14 (Fig. 4.3B).

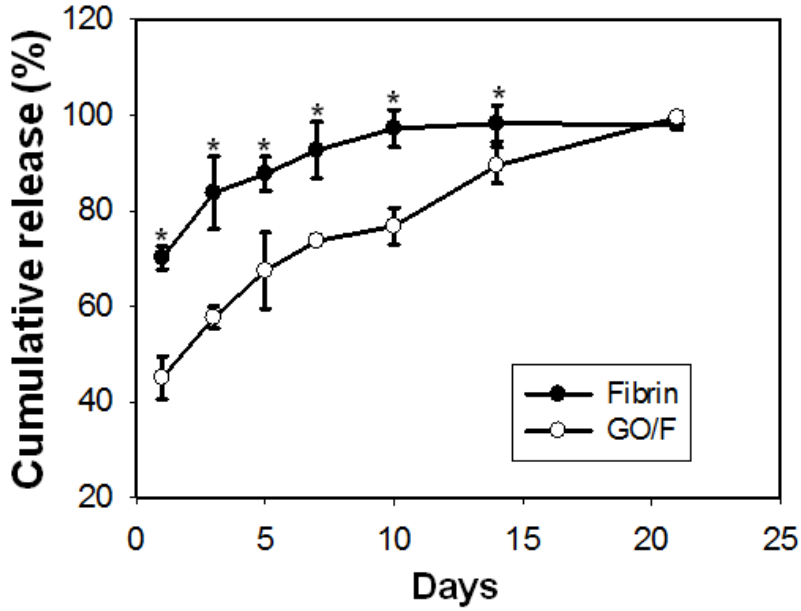

Figure 4.1. Sustained release of BMP-2 from GO/F versus F. The BMP-2 release kinetics were determined by ELISA (n = 5). * $p < 0.05$.

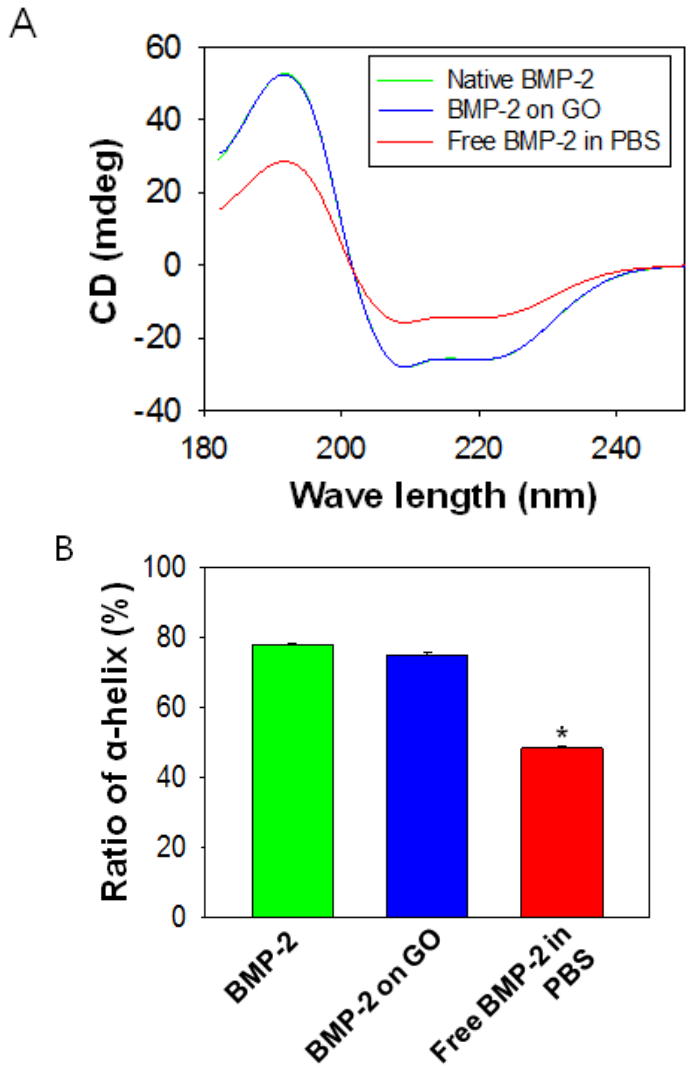

Figure 4.2. Higher structural stability of BMP-2 delivered by GO. (A) Superior structural stability of BMP-2 adsorbed on GO in PBS on day 3, compared to free BMP-2 in PBS on day 3, as evaluated by circular dichroism. (B) The ratio of α-helix in BMP-2, as evaluated by structural analysis on day 3 using circular dichroism.

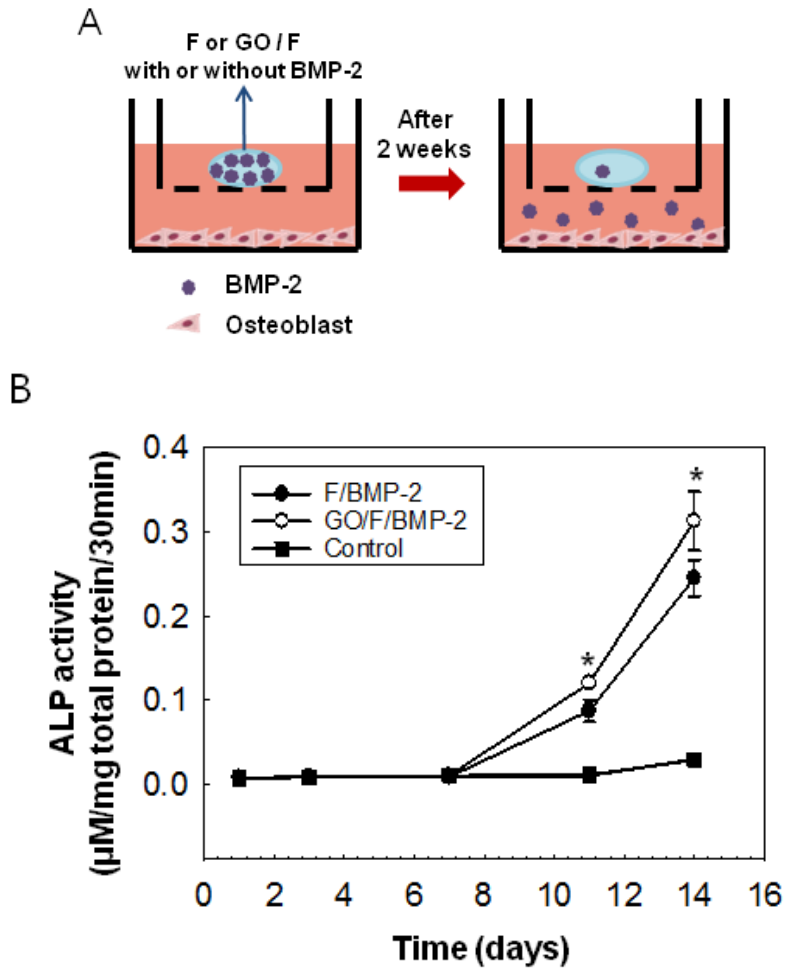

Figure 4.3. Higher bioactivity of BMP-2 delivered by GO. (A) Transwell culture system to evaluate the bioactivity of BMP-2 released from the carriers by determining (B) ALP activity of rat calvarial osteoblasts cultured with different delivery systems (n = 3, * $p < 0.05$ versus F/BMP-2). The control group was not supplemented with BMP-2.

3.5. In vitro osteogenic differentiation of hBMMSCs by released BMP-2

The in vitro osteogenic differentiation efficacy of BMP-2 delivered by GO/F or F was investigated by evaluating the osteogenic differentiation of hBMMSCs cultured in the presence of BMP-2 released from the carriers. Immunocytochemical staining showed that the expression of OC, an osteogenic differentiation marker [14,16,29], was higher in the GO/F/BMP-2 group compared with the F/BMP-2 group (Fig. 5.1A). qRT-PCR analysis also showed significantly higher mRNA expression of an early osteogenic marker (ALP) and late osteogenic markers (OC and osteopontin (OP)) in hBMMSCs in the GO/F/BMP-2 group compared with the F/BMP-2 group (Fig. 5.1B).

The ability of BMP-2 delivered by GO/F to upregulate cell signaling related to the osteogenic differentiation of hBMMSCs was investigated. Bioactive BMP-2 induces the phosphorylation of Smad 1/5/8 (to form p-Smad 1/5/8) in hBMMSCs [29]. BMP-2 released from GO/F induced more robust phosphorylation of Smad 1/5/8 than did BMP-2 released from F (Fig. 5.2).

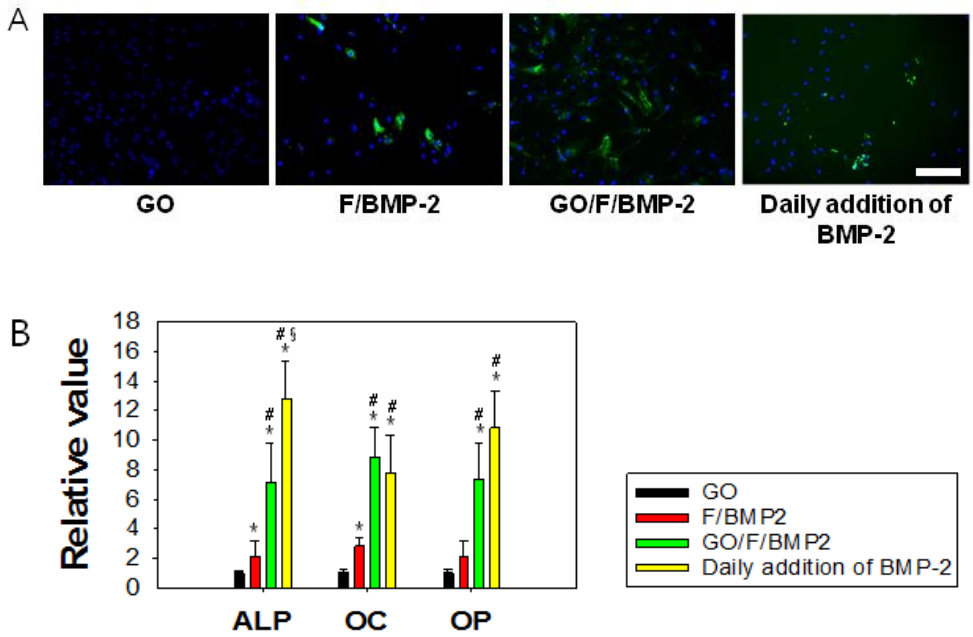

Figure 5.1. Enhanced in vitro osteogenic differentiation of hBMMSCs cultured in the presence of BMP-2 released from GO/F. (A) Immunocytochemical staining for osteocalcin (OC, green), an osteogenic differentiation marker, in hBMMSCs cultured for 2 weeks with different delivery systems. Daily addition of BMP-2 to medium served as a positive control. The cell nuclei were counterstained with DAPI (blue). Scale bars = 10 μm. (B) qRT-PCR analysis to detect the mRNA expression of an early osteogenic differentiation marker (ALP) and late osteogenic markers (OC and OP) in hBMMSCs at 2 weeks (n = 5, * $p < 0.05$ versus GO, # $p < 0.05$ versus F/BMP-2, § $p < 0.05$ versus GO/F/BMP-2).

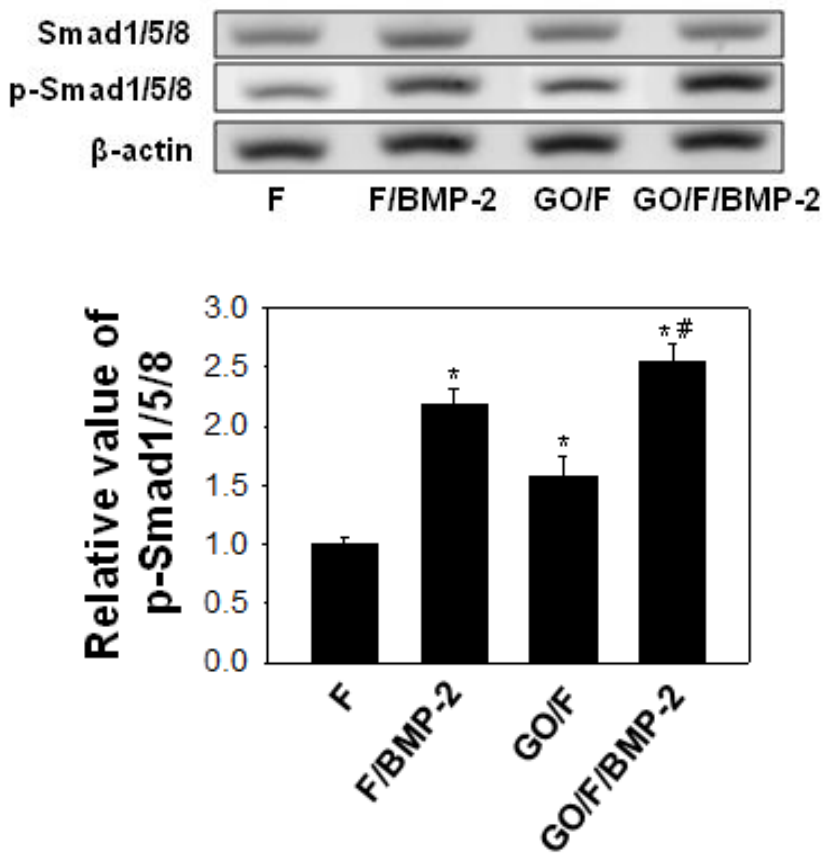

Figure 5.2. Enhanced cell signaling related to osteogenic differentiation of hBMMSCs by BMP-2 delivered by GO, as evaluated by western blotting. Bioactive BMP-2 induces Smad 1/5/8 phosphorylation in hBMMSCs. n = 3, * $p < 0.05$ versus F, # $p < 0.05$ versus F/BMP-2.

3.6 In vivo bone formation

The ability of BMP-2 delivered using GO/F to reduce the BMP-2 dose required for in vivo bone formation was investigated. The in vivo bone formation efficacy of BMP-2 depended on the carrier; micro-CT examination (Fig. 6.1) and histological analysis with Goldner's trichrome staining (Fig. 6.2) showed that the delivery of various doses of BMP-2 using GO/F resulted in significantly greater bone regeneration than that using F in mouse calvarial defects. The bone formation increased with the dose of BMP-2 in both groups. No bone formation was observed in the groups without BMP-2 at 8 weeks. Mature bone with lamellar structures and osteocytes in lacunae was observed in the new bone tissues. The bone formation area in the 0.5 μg BMP-2/GO/F group was approximately equal to that in the 1.0 μg BMP-2/F group, indicating that a half-dose of BMP-2 delivered by GO/F resulted in bone formation similar to that resulting from a full dose of BMP-2 delivered by F.

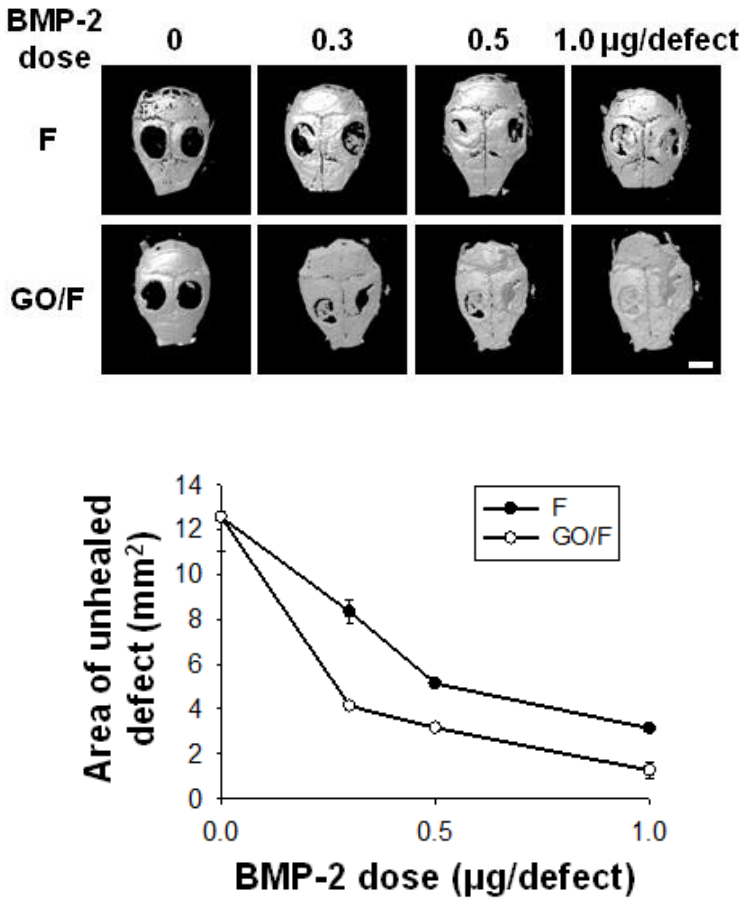

Figure 6.1. Bone regeneration evaluated by micro-CT. Representative micro-CT images of mouse skulls. Mouse calvarial defects were treated with various doses of BMP-2 delivered by either F or GO/F for 8 weeks. The defects were treated with 0, 0.3, 0.5, and 1.0 µg BMP-2 per defect. Scale bars = 4 mm. The area of unhealed defect was determined from the micro-CT images. n = 10 defects per group.

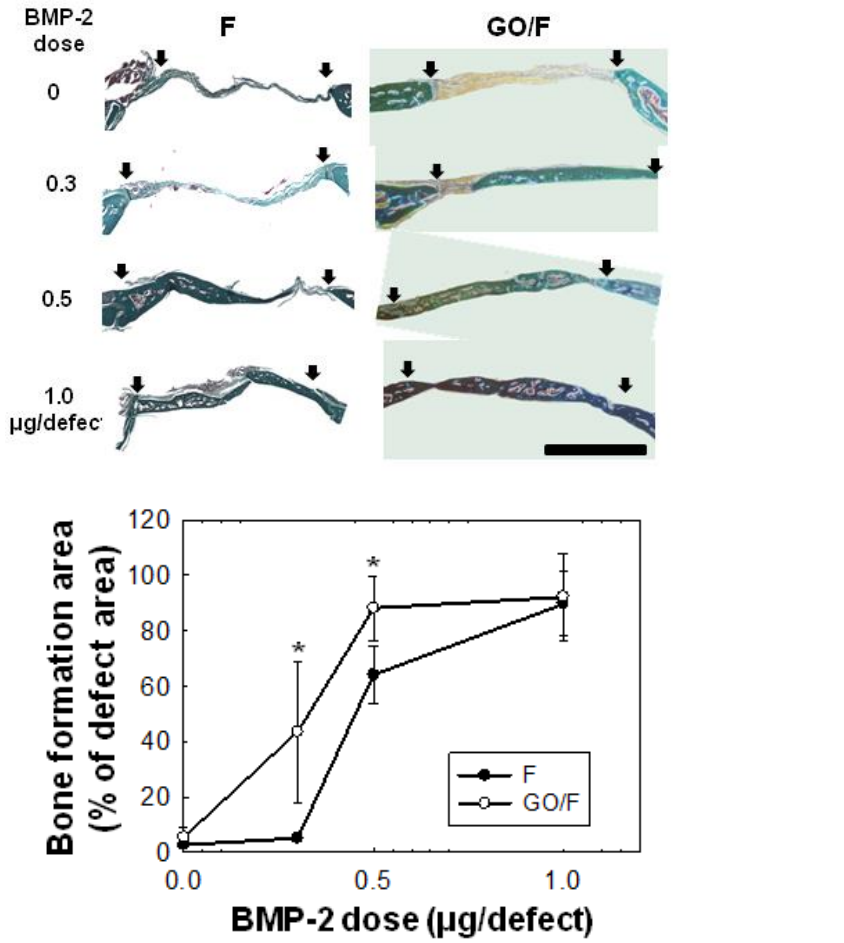

Figure 6.2. Bone regeneration evaluated by histological analysis with Goldner's trichrome staining of mouse calvarial defects. Mouse calvarial defects were treated with various doses of BMP-2 delivered by either F or GO/F for 8 weeks. Arrows indicate the defect margins. Scale bars = 2 mm. All photographs were taken at 40x magnification. The area of new bone was determined by histomorphometric analysis (n = 10 defects, * $p < 0.05$ between two groups).

4. Discussion

As a BMP-2 delivery vehicle, GO exerted a sustained release of BMP-2 and maintained its bioactivity, which is important for bone regeneration. GO adsorbs BMP-2 effectively (Fig. 3.1, 3.2) through the electrostatic interaction between the negatively charged domains of GO and the positively charged BMP-2 [21] and the interaction between π-electron clouds in GO's carbon and the inner hydrophobic cores of the BMP-2 protein [23,28,30]. These interactions may also contribute to the sustained release of BMP-2 (Fig. 3.1, 3.2). The higher bioactivity of BMP-2 released from GO, compared with that of free BMP-2, is likely due to the conformational stability of BMP-2 adsorbed on GO.

The enhanced in vitro osteogenic activity and in vivo bone regeneration efficacy of BMP-2 in the GO/F/BMP-2 group may be due to the sustained release, higher structural stability, and higher bioactivity of BMP-2 delivered by GO/F. Long-term release of BMP-2 in a bioactive form has been shown to increase its bone formation efficacy [11,12,17,21]. It was reported that the long-term release of BMP-2 over 4 weeks induced a higher degree of bone formation compared with the same amount of BMP-2 released over 3 days [18,31]. Other studies also reported that BMP-2 release over fewer than 7 days did not induce a significant amount of bone formation [32,33]. The long-term delivery of BMP-2 promotes the migration and osteogenic differentiation of stem cells or progenitor cells, which are required for successful bone formation. Long-term delivery of BMP-2 can enhance the migration of osteogenic progenitor cells from the bone defect margin to the defect site for bone formation [34]. Long-term delivery of BMP-2 can enable osteogenic differentiation of stem cells or progenitor cells, which takes several weeks [35]. Our previous study showed that BMP-2 adsorbed on GO was protected from

protein denaturation and was released in a bioactive form [21]. The enhanced in vivo bone regeneration may not be attributed to the good mechanical properties of GO, since the mechanical properties of F and GO/F were not significantly different (Fig. S3).

The F in GO/F can localize the GO in the bone defect sites and can also play the role of scaffold for bone formation. It is difficult to localize GO sheets at bone defect sites because GO has a sheet-like form with an average size of 1.8 μm (Fig. 1). In addition, GO sheets cannot provide three-dimensional space for bone formation. GO sheets can be suspended in F and easily injected into bone defects, which would facilitate the localization of GO in the bone defects. F has been successfully used as a scaffold for bone tissue engineering [11,14]. Injectable F can be easily used to fill bone defects of any shape. F degrades more than 90 % in vivo within 9 days [29] , thus permitting the efficient filling of bone defects with regenerated bone and leading to higher bone density. GO is known to be hardly degradable without specific enzyme treatment [36]. However, it may not cause a problem for bone regeneration applications if the GO is used at non-toxic, low concentrations. The concentration of GO used in our experiment (1 μg/ml) was far less than the amount of GO that was reported as cytotoxicity previously (1 mg/ml) [25]. As a comparative example, hydroxyapatite, which is widely used for bone regeneration, degrades very slowly and has not been reported for any side effects induced by residues remained after in vivo implantation.

The bone formation efficacy of BMP-2 delivered by GO/F was superior to those of BMP-2 delivered by other delivery systems. A half-dose (0.5 μg) of BMP-2 delivered using GO/F showed bone formation efficacy similar to a full dose (1.0 μg) of BMP-2 delivered with F (Fig. 6.1, 6.2). In the same animal model (six-

week-old Institute of Cancer Research mice) with the same defect size and treatment period, delivery of 0.5 μg and 1.0 μg of BMP-2 by GO/F resulted in bone formation areas of 88 % and 90 %, respectively (Fig. 6.2), whereas delivery of the same doses of BMP-2 by heparin-conjugated PLGA nanospheres suspended in F resulted in bone formation areas of 25 % and 67 %, respectively [18]. Importantly, with the increased bone formation efficacy of BMP-2, the GO/F system can reduce the dose of BMP-2 necessary for successful bone formation and help avoid or diminish the potential adverse effects elicited by the excessive administration of BMP-2, which can occur with other delivery systems.

5. Conclusions

BMP-2 delivery using GO/F promoted greater osteogenic differentiation of hBMMSCs in vitro and more bone regeneration in vivo than BMP-2 delivery using F. Importantly, delivery of BMP-2 using GO can reduce the BMP-2 dose required for bone regeneration. A half-dose of BMP-2 delivered by GO/F promoted bone regeneration similar to that resulting from a full dose of BMP-2 delivered by F, which may be due, at least in part, to the sustained release, higher structural stability, and higher bioactivity of BMP-2 delivered by GO/F. Therefore, GO may be an effective carrier for BMP-2 delivery, which can reduce the required BMP-2 dose and the adverse effects caused by high doses of BMP-2.

References

[1] Reddi AH. BMPs: from bone morphogenetic proteins to body morphogenetic proteins. Cytokine Growth Factor Rev 2005;16(3):249-50.

[2] Termaat MF, Den Boer FC, Bakker FC, Patka P, Haarman HJ. Bone morphogenetic proteins. Development and clinical efficacy in the treatment of fractures and bone defects. J Bone Joint Surg Am 2005;87(6):1367-78.

[3] Govender S, Csimma C, Genant HK, Valentin-Opran A, Amit Y, Arbel R, et al. Recombinant human bone morphogenetic protein-2 for treatment of open tibial fractures: a prospective, controlled, randomized study of four hundred and fifty patients. J Bone Joint Surg Am 2002;84-A(12):2123-34.

[4] Gautschi OP, Frey SP, Zellweger R. Bone morphogenetic proteins in clinical applications. ANZ J Surg 2007;77(8):626-31.

[5] Poynton AR, Lane JM. Safety profile for the clinical use of bone morphogenetic proteins in the spine. Spine 2002;27(16S):S40-8.

[6] Shields LB, Raque GH, Glassman SD, Campbell M, Vitaz T, Harpring J, et al. Adverse effects associated with high-dose recombinant human bone morphogenetic protein-2 use in anterior cervical spine fusion. Spine 2006;31(5):542-7.

[7] Mont MA, Ragland PS, Biggins B, Friedlaender G, Patel T, Cook S, et al. Use of Bone Morphogenetic Proteins for Musculoskeletal Applications. An Overview. J Bone Joint Surg Am 2004;86(Suppl 2):41-55.

[8] Carragee EJ, Hurwitz EL, Weiner BK. A critical review of recombinant human bone morphogenetic protein-2 trials in spinal surgery: emerging safety concerns and lessons learned. Spine J 2011;11(6):471-91.

[9] Lewandrowski KU, Nanson C, Calderon R. Vertebral osteolysis after posterior interbody lumbar fusion with recombinant human bone morphogenetic protein 2: a report of five cases. Spine J 2007;7(5):609-14.

[10] Wong DA, Kumar A, Jatana S, Ghiselli G, Wong K. Neurologic impairment from ectopic bone in the lumbar canal: a potential complication of off-label PLIF/TLIF use of bone morphogenetic protein-2 (BMP-2). Spine J 2008;8(6):1011-8.

[11] Yang HS, La WG, Bhang SH, Jeon JY, Lee JH, Kim BS. Heparin-Conjugated Fibrin as an Injectable System for Sustained Delivery of Bone Morphogenetic Protein-2. Tissue Eng Part A 2010;16(4):1225-33.

[12] Yamamoto M, Takahashi Y, Tabata Y. Enhanced bone regeneration at a segmental bone defect by controlled release of bone morphogenetic protein-2 from a biodegradable hydrogel. Tissue Eng 2006;12(5):1305-11.

[13] Friess W, Uludag H, Foskett S, Biron R, Sargeant C. Characterization of absorbable collagen sponges as recombinant human bone morphogenetic protein-2 carriers. Int J Pharm 1999;185(1):51-60.

[14] La WG, Kwon SH, Lee TJ, Yang HS, Park J, Kim BS. The effect of the delivery carrier on the quality of bone formed via bone morphogenetic protein-2. Artif Organs 2012;36(7):642-7.

[15] Noshi T, Yoshikawa T, Ikeuchi M, Dohi Y, Ohgushi H, Horiuchi K, et al. Enhancement of the in vivo osteogenic potential of marrow/hydroxyapatite composites by bovine bone morphogenetic protein. J Biomed Mater Res 2000;52(4):621-30.

[16] Jeon O, Rhie JW, Kwon IK, Kim JH, Kim BS, Lee SH. In vivo bone formation following transplantation of human adipose-derived stromal cells that are not differentiated osteogenically. Tissue Eng Part A 2008;14(8):1285-94.

[17] Jeon O, Song SJ, Kang SW, Putnam AJ, Kim BS. Enhancement of ectopic bone formation by bone morphogenetic protein-2 released from a heparin-conjugated poly (L-lactic-co-glycolic acid) scaffold. Biomaterials 2007;28(17):2763-71.

[18] La WG, Kang SW, Yang HS, Bhang SH, Lee SH, Park JH, et al. The efficacy of bone morphogenetic protein-2 depends on its mode of delivery. Artif Organs 2010;34(12):1150-3.

[19] Feng L, Zhang S, Liu Z. Graphene based gene transfection. Nanoscale 2011;3(3):1252-7.

[20] Zhang W, Guo Z, Huang D, Liu Z, Guo X, Zhong H. Synergistic effect of chemo-photothermal therapy using PEGylated graphene oxide. Biomaterials 2011;32(33):8555-61.

[21] La WG, Park S, Yoon HH, Jeong GJ, Lee TJ, Bhang SH, et al. Delivery of a therapeutic protein for bone regeneration from a substrate coated with graphene oxide. Small 2013;3(23):4051-60.

[22] Nayak TR, Andersen H, Makam VS, Khaw C, Bae S, Xu X, et al. Graphene for controlled and accelerated osteogenic differentiation of human mesenchymal stem cells. ACS Nano 2011;5(6):4670-8.

[23] Lee WC, Lim CH, Shi H, Tang LA, Wang Y, Lim CT, et al. Origin of enhanced stem cell growth and differentiation on graphene and graphene oxide. ACS Nano 2011;5(9):7334-41.

[24] Repetto G, del Peso A, Zurita JL. Neutral red uptake assay for the estimation of cell viability/cytotoxicity. Nat Protoc 2008;3(7):1125-31.

[25] Kim J, Choi KS, Kim Y, Lim KT, Seonwoo H, Park Y, et al. Bioactive effects of graphene oxide cell culture substratum on structure and function of human adipose-derived stem cells. J Biomed Mater Res A 2013;101(12):3520-30.

[26] Yue H, Wei W, Yue Z, Wang B, Luo N, Gao Y, et al. The role of the lateral dimension of graphene oxide in the regulation of cellular responses. Biomaterials 2012;33(16):4013-21.

[27] Lee JH, Kim CS, Choi KH, Jung UW, Yun JH, Choi SH, et al. The induction of bone formation in rat calvarial defects and subcutaneous tissues by recombinant human BMP-2, produced in Escherichia coli. Biomaterials 2010;31(13):3512-9.

[28] Zhang Z, Zhang J, Zhang B, Tang J. Mussel-inspired functionalization of graphene for synthesizing Ag-polydopamine-graphene nanosheets as antibacterial materials. Nanoscale 2013;5(1):118-23.

[29] Yang HS, La WG, Bhang SH, Kim HJ, Im GI, Lee H, et al. Hyaline cartilage regeneration by combined therapy of microfracture and long-term bone morphogenetic protein-2 delivery. Tissue Eng Part A 2011;17(13-14):1809-18.

[30] Utesch T, Daminelli G, Mroginski MA. Molecular dynamics simulations of the adsorption of bone morphogenetic protein-2 on surfaces with medical relevance. Langmuir 2011;27(21):13144-53.

[31] Jeon O, Song SJ, Yang HS, Bhang SH, Kang SW, Sung MA, et al. Long-term delivery enhances in vivo osteogenic efficacy of bone morphogenetic protein-2 compared to short-term delivery. Biochem Biophys Res Commun 2008;369(2):774-80.

[32] Uludag H, Gao T, Porter TJ, Friess W, Wozney JM. Delivery systems for BMPs: Factors contributing to protein retention at an application site. J Bone Joint Surg Am 2001;83(1 Suppl 2):S128-35.

[33] Boerckel JD, Kolambkar YM, Dupont KM, Uhrig BA, Phelps EA, Stevens HY, et al. Effects of protein dose and delivery system on BMP-mediated bone regeneration. Biomaterials 2011;32(22):5241-51.

[34] Issa JP, Bentley MV, Iyomasa MM, Sebald W, De Albuquerque RF. Sustained release carriers used to delivery bone morphogenetic proteins in the bone healing process. Anat Histol Embryol 2008;37(3):181-7.

[35] Huang W, Carlsen B, Wulur I, Rudkin G, Ishida K, Wu B, et al. BMP-2 exerts differential effects on differentiation of rabbit bone marrow stromal cells grown in two-dimensional and three-dimensional systems and is required for in vitro bone formation in a PLGA scaffold. Exp Cell Res 2004;299(2):325-34.

[36] Kotchey GP, Allen BL, Vedala H, Yanamala N, Kapralov AA, Tyurina YY, et al. The enzymatic oxidation of graphene oxide. ACS Nano 2011;5(3):2098-108.

Supplementary data

S1. Supplementary data experimental

S1.1. Loading efficiency and release kinetics of bone morphogenic protein (BMP)-2 with various GO conditions

The loading efficiency of BMP-2 at two different weight ratios of BMP-2 to GO (1:0.1 or 1:1), or GO with different oxidation degrees was determined by enzyme-linked immunosorbent assays (ELISAs, R&D Systems Inc., Minneapolis, MN, USA) [1]. The GOs were dispersed in 1 ml of phosphate buffered saline (PBS) with 1 μg of BMP-2 in each microcentrifuge tube and incubated for 4 h at 4 ℃. The suspensions were centrifuged at 10,000 g for 5 min to collect the supernatants. The concentration of BMP-2 in the supernatants was determined by ELISA. The loading efficiency of BMP-2 on various types of GOs was calculated according to the following equation:

$$\text{Loading efficiency (\%)} = \frac{Co - C}{Co} \times 100\ \%$$

[*Co*: initial concentration of BMP-2, *C*: BMP-2 concentration in supernatant (unit: μg/ml)].

The release profiles of BMP-2 from GO/F and GO with fibrin gel loaded with GO after reduction process (reduced GO/F) were determined by ELISAs [1]. To determine the BMP-2 release from GO, 1 μg of BMP-2 was added to 20 μl of PBS and attached to GO (20 μg/ml fibrin) or reduced GO (20 μg/ml fibrin) for 4 h at 4 ℃. F kits (Greenplast®) were purchased from GreencrossPD Co. (Yongin, South Korea). F was prepared by mixing fibrinogen (100 mg/ml) dissolved in aprotinin (100 KIU/ml) solution with thrombin (500 IU) dissolved in calcium

chloride solution (6 mg/ml). The BMP-2-loaded GO and reduced GO for different oxidation was suspended in 50 μl of F and immersed in a 1.7-ml microcentrifuge tube containing 1 ml of PBS. The tubes were then incubated at 37 ℃ with continuous agitation. At various time points, the supernatant was collected, and fresh buffer was added to the microcentrifuge tubes. The concentration of BMP-2 in the supernatant was determined by ELISA.

S1.2. The compressive elastic modulus of F and GO/F

The F or GO/F samples collected for evaluating compressive elastic modulus. The samples were cylinder shape with dimensions of 10 mm diameter × 5 mm anvil height. The samples were immersed in PBS for 24 h at 37 ℃ before measurement. Compressive elastic modulus of F or GO/F was investigated with a universal testing machine (UTM, Instron 5543, MA, USA) at 25 ℃. F or GO/F was compressed with a constant deformation rate of 1 mm min^{-1}. Compressive elastic modulus of F or GO/F was calculated from the slope of stress vs. strain curves, limited to the first 10 % of strain.

S2. Supplementary data figures

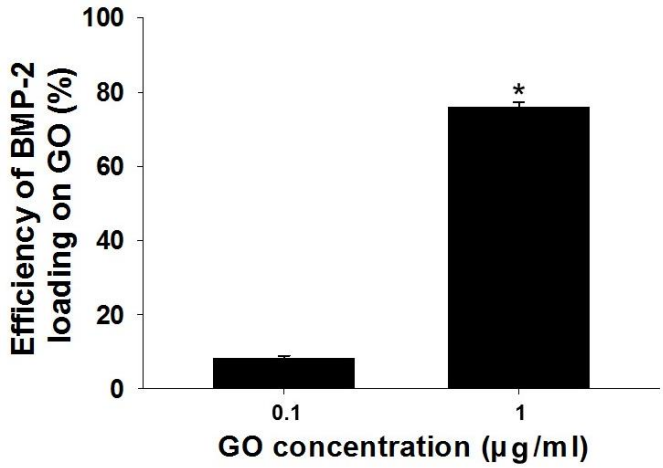

Supplementary data figure 1. The BMP-2 loading efficiency on GO at two weight ratios of BMP-2 to GO, as determined by ELISA (N = 3). One μg of BMP-2 was loaded on 0.1 μg (the weight ratio of BMP-2 to GO = 1:0.1) or 1 μg (the weight ratio of BMP-2 to GO = 1:1) of GO. * $p < 0.05$ compared to the other group.

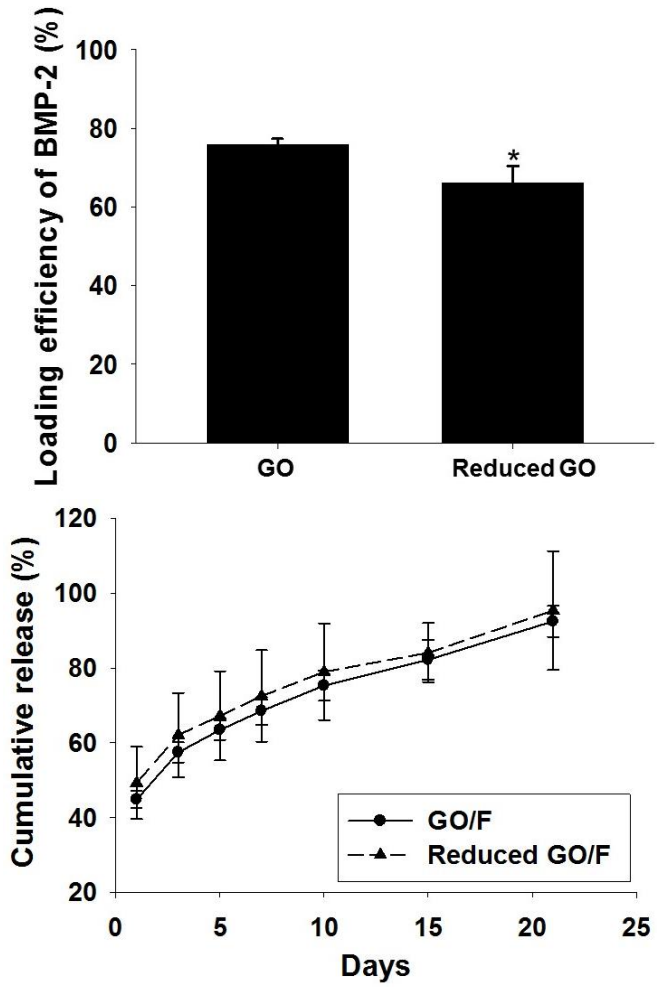

Supplementary data figure 2. The BMP-2 loading efficiency on GO at two different oxidation degrees (left, N = 3) and BMP-2 release kinetics from GO at two oxidation degrees (right, N = 3) as determined by ELISA. * $p < 0.05$ compared to the other group.

s

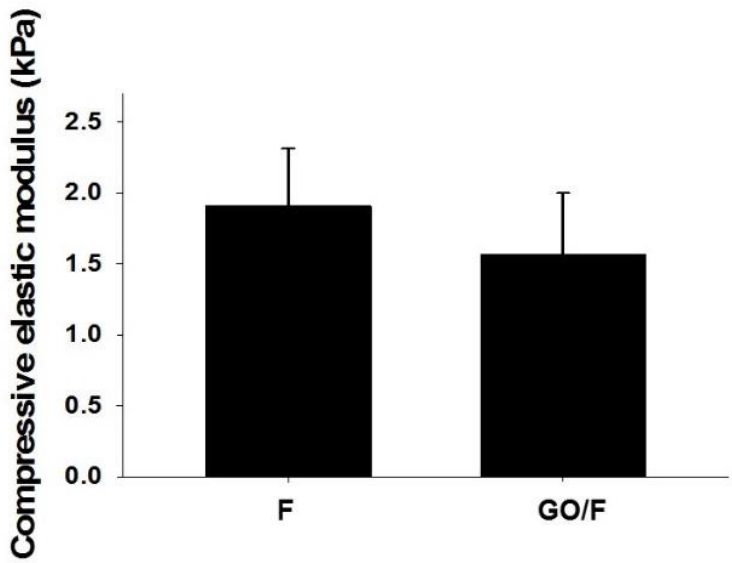

Supplementary data figure 3. Compressive elastic modulus of F and GO/F. No significant differences were observed between two groups. Universal testing machine was used to measure the compressive elastic modulus.

S3. Supplementary data references

[1] Carragee EJ, Hurwitz EL, Weiner BK. A critical review of recombinant human bone morphogenetic protein-2 trials in spinal surgery: emerging safety concerns and lessons learned. Spine J 2011;11(6):471-91.

요약 (국문초록)

그래핀 옥사이드 기반의 약물 전달을 통한 골형성 단백질 용량 감소 및 뼈 재생

효과적인 골 재생을 위해서는 고용량의 골형성 단백질 (BMP-2)이 필요하다. 하지만 고용량의 BMP-2 사용은 골 과다 형성, 골 용해, 면역 반응 유발 등의 부작용들을 야기할 수 있으며, 치료 비용을 증가시킬 수 있다. 본 연구에서는 위와 같은 BMP-2 고용량 사용에 의한 부작용을 줄이기 위하여, 그래핀 옥사이드 (GO) 기반의 BMP-2 전달을 통한 BMP-2 용량 감소 및 골 재생을 연구하였다. 피브린 젤 속에 부유하는 GO 박편 (GO/F)을 이용하여 BMP-2 를 전달한 결과, 피브린 젤 (F)만을 이용한 BMP-2 전달에 비하여 생체 외 배양 조건에서 인간 골수 유래 중간엽줄기세포의 골분화가 효과적으로 향상 되었다. 또한 마우스 두개골 결손 모델에서 다양한 농도의 BMP-2 를 사용하여 실험한 결과, F 를 이용한 BMP-2 전달에 비하여 GO/F 를 이용한 BMP-2 전달에서 더 많은 양의 골 재생이 이루어졌다. 그리고 F 를 이용한 정상용량의 BMP-2 전달과 GO/F 를 이용한 정상용량의 1/2 의 BMP-2 전달에서 유사한 정도의 골 재생을 보였다. F 를 이용한 BMP-2 전달과 비교하였을 때, GO/F 를 이용한 BMP-2 전달의 향상된 골 재생 효과는 BMP-2 의 서방 방출, 높은 구조적 안정성 유지, 높은 생물 작용성 유지에 의한

것으로 생각된다. 그러므로, GO 를 이용하여 BMP-2 를 전달함으로써 BMP-2 의 용량을 감소하고 부작용을 줄일 수 있을 것으로 생각된다.

주요어: 골 형성 단백질, 골 재생, 피브린 젤, 그래핀 옥사이드

학번: 2013-21041